Nonlocal Treatment of the Buoyancy-Shear-Driven Boundary Layer

E. FERRERO AND N. COLONNA

Dipartimento di Scienze e Tecnologie Avanzate, Università del Piemonte Orientale, Alessandria, Italy

(Manuscript received 25 July 2005, in final form 2 December 2005)

ABSTRACT

A successful description of a convective boundary layer requires that the model employed takes into account the nonlocal nature of turbulent convection. In this paper new third-order moments (TOMs) are presented and tested. Numerical solutions are obtained using mean flow components and second-order moments as input. The problem of the turbulent damping of the TOMs is considered. The terms in the dynamic equations responsible for the unphysical growth of the TOMs are parameterized, taking into account their dependence on the integral length scale vertical profile. The calculated profiles are presented and tested against large-eddy simulation data and aircraft measurements. In both cases the results compare favorably.

1. Introduction

Within the boundary layer (BL) turbulence is generated and maintained by shear and buoyancy. An important feature of convective boundary layer (CBL) is the presence of large-scale semiorganized structures (large-scale implies that the structure's spatial scale is comparable to the CBL depth). The nonlocal nature of vertical transport of potential temperature (buoyancy), momentum, and passive scalars across the CBL is essentially due to these structures. The models used to describe such atmospheric flows can be roughly classified into two categories. The first one is represented by local models (e.g., Mellor and Yamada 1974, 1982; Canuto and Cheng 1994; Canuto et al. 2002; Abdella and McFarlane 1997; Trini Castelli et al. 2001) in which the third-order moments (TOMs) are neglected and all fluxes are determined by vertical local gradients of the mean wind and mean potential temperature. It is known that these models fail when applied to convective flows (Moeng and Wyngaard 1989) since they considerably underestimate the TOMs and produce insufficient vertical transport, thus predicting the maxima of the relative humidity and the cloud height closer to the surface than the observations (e.g., Holstag and Boville 1993). The improvements of these models (e.g., Deardorff 1972; Holstag and Moeng 1991; Wyngaard and Weil 1991; Canuto et al. 2005) include nonlocal terms but do not resolve dynamic equations for the TOMs and, thus, the results, especially for convective flows, are not completely satisfactory. Thus, one must overcome these limitations and employ models that contain dynamic equations for the third-order moments, that is, nonlocal models (e.g., Canuto 1992; Canuto et al. 1994; Zilitinkevich et al. 1999; Canuto et al. 2001; Cheng et al. 2005; Ferrero and Racca 2004; Ferrero 2005; Gryanik et al. 2005).

Recently Ferrero and Racca (2004) showed that the nonlocal transport plays an important role, not only in the case of CBL, but also in the case of pure shear BL. They demonstrated that a model including TOMs is able to better determine the BL height in the neutral case, even though such flows are not characterized by such large-scale structures, as in the case of convective flows. Therefore it is essential that a turbulence model for the shear-buoyancy BL takes into account the nonlocal transport.

Canuto (1992) proposed a new complete model for the TOMs, including shear, buoyancy, rotation, and overshooting that is capable of describing pure convective boundary layer as assessed in Canuto et al. (2001). This model was also successfully applied by Ferrero (2005), who carried out a satisfactory comparison of the TOM model with the prediction of large-eddy simula-

Corresponding author address: Dr. Enrico Ferrero, Dipartimento di Scienze e Tecnologie Avanzate, Università del Piemonte Orientale, v. Bellini 25/G, Alessandria 15100, Italy.
E-mail: enrico.ferrero@unipmn.it

tion (LES) results by Moeng and Sullivan (1994) for a pure shear BL.

In general, the most studied cases are, for the sake of simplicity, the neutral BL, and the pure convective flow. Here we consider a flow with both shear and convection that represent a more realistic atmospheric boundary layer. A similar flow was considered by Gryanik and Hartmann (2002), but in that paper the closure problem for the convective turbulence of the shear-free and weakly sheared atmospheric BL is investigated with the mass-flux approach.

Experimental studies of the atmospheric CBL with measurements of higher-order moments of the turbulence were performed by Lenschow (1974) and Lenschow et al. (1980). In these works aircraft measurements of the turbulent kinetic energy, temperature and humidity budgets, turbulent kinetic energy, and potential temperature variance vertical fluxes are shown. A comparison between LES simulations and atmospheric data is provided by Moeng and Rotunno (1990). In that paper, they demonstrated that the TOMs simulated by LES and those measured in the atmosphere can show different behavior. Thus, to test a turbulence model it is essential to consider both LES and field experiments.

In this work, we first use LES data by Moeng and Sullivan (1994) to investigate the case of a buoyancy-dominated flow with a relatively small shear effect (Moeng and Sullivan 1994, case B). We consider a horizontally homogeneous BL. The dynamic equations for the TOMs are derived following Canuto (1992), numerically solved and tested against LES data. We also used to test our results aircraft measurements taken during the Arctic Radiation and Turbulence Interaction Study (ARTIST) campaign in the polar convective boundary layer during a cold air outbreak over the ocean at moderate wind (Hartmann et al. 1999). Then, in order to verify the general validity of our approach, we compare our model with the case SB1 of Moeng and Sullivan (1994), which is characterized by both shear and buoyancy.

In section 2 the dynamic equations system and other model settings are presented. In section 3 the problem of the turbulent damping for the TOMs is discussed and a new approach to avoid the unphysical growth of the TOMs is suggested. Finally, in section 4, the model results are presented and tested against LES data and aircraft measurements.

2. Third-order moments

Since the dynamic equations for the third order moments entail fourth-order moments (FOMs), a proper parameterization of the FOMs is required. The TOM fluxes are expressed in term of second-order correlations (Hanjalic and Launder 1972, 1976; Zeman 1981):

$$\overline{abcd} = \overline{ab}\,\overline{cd} + \overline{ac}\,\overline{bd} + \overline{ad}\,\overline{bc}. \tag{1}$$

Following Canuto (1992), the resulting system of 20 dynamic equations, in horizontally homogeneous conditions, is given by

$$\left(\frac{\partial}{\partial t} + \tau_3^{-1}\right)\overline{u_i u_j u_k} = -\left(\overline{u_i u_j u_3}\frac{\partial U_k}{\partial x_3} + \overline{u_k u_i u_3}\frac{\partial U_j}{\partial x_3} + \overline{u_j u_k u_3}\frac{\partial U_i}{\partial x_3}\right) - \left(\overline{u_i u_3}\frac{\partial}{\partial x_3}\overline{u_j u_k} + \overline{u_k u_3}\frac{\partial}{\partial x_3}\overline{u_i u_j} + \overline{u_j u_3}\frac{\partial}{\partial x_3}\overline{u_k u_i}\right) + (1 - c_{11})(\lambda_i\overline{\theta u_j u_k} + \lambda_j\overline{\theta u_k u_i} + \lambda_k\overline{\theta u_i u_j}) - \frac{2}{3\tau}(\delta_{ij}\overline{q^2 u_k} + \delta_{3j}\overline{q^2 u_i} + \delta_{jk}\overline{q^2 u_i}), \tag{2}$$

$$\left(\frac{\partial}{\partial t} + \tau_3^{-1}\right)\overline{u_i u_j \theta} = -\overline{u_i u_j u_3}\frac{\partial \Theta}{\partial x_3} - \left(\overline{u_i u_3 \theta}\frac{\partial U_j}{\partial x_3} + \overline{u_j u_3 \theta}\frac{\partial U_i}{\partial x_3}\right) - \left(\overline{u_i u_3}\frac{\partial}{\partial x_3}\overline{\theta u_j} + \overline{u_j u_3}\frac{\partial}{\partial x_3}\overline{\theta u_i} + \overline{\theta u_3}\frac{\partial}{\partial x_3}\overline{u_i u_j}\right) + (1 - c_{11})(\lambda_i\overline{\theta^2 u_j} + \lambda_j\overline{\theta^2 u_i}) + \frac{2}{3}c_{11}\delta_{ij}\lambda_k\overline{\theta^2 u_k} + \frac{c_*}{\tau}\delta_{ij}\overline{q^2\theta}, \tag{3}$$

$$\left(\frac{\partial}{\partial t} + \tau_3^{-1} + 2\tau_\theta^{-1}\right)\overline{u_i\theta^2} = -2\overline{\theta u_i u_3}\frac{\partial \Theta}{\partial x_3} - \overline{u_3\theta^2}\frac{\partial U_i}{\partial x_3} - 2\overline{u_3\theta}\frac{\partial}{\partial x_3}\overline{\theta u_i} + (1 - c_{11})\lambda_i\overline{\theta^3} - \overline{u_i u_3}\frac{\partial}{\partial x_3}\overline{\theta^2}, \tag{4}$$

$$\left(\frac{\partial}{\partial t} + \frac{c_{10}}{c_8}\tau_3^{-1}\right)\overline{\theta^3} = -3\overline{\theta^2 u_3}\frac{\partial \Theta}{\partial x_3} - 3\overline{u_3\theta}\frac{\partial}{\partial x_3}\overline{\theta^2}, \tag{5}$$

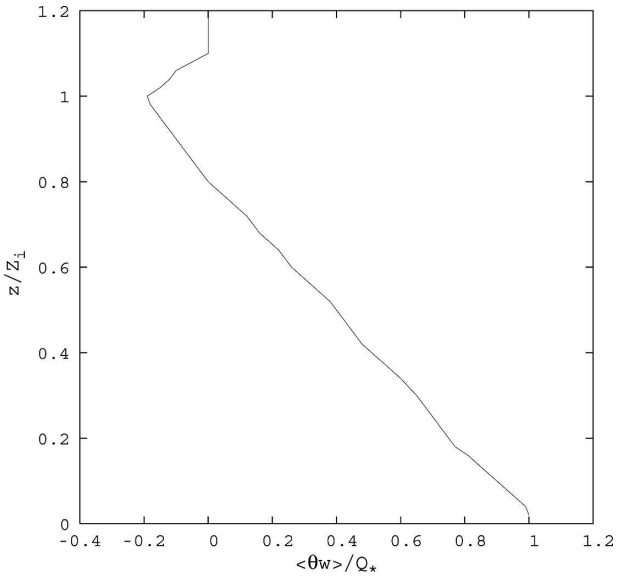

FIG. 1. Vertical profile of the normalized convective heat flux $\overline{w\theta}$.

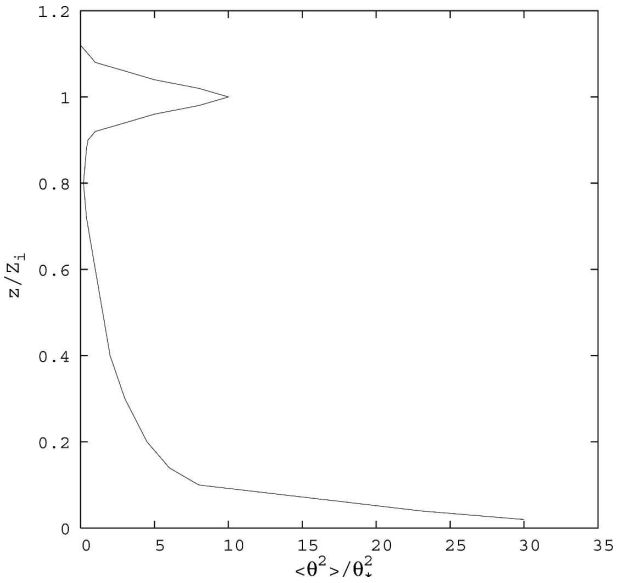

FIG. 2. Vertical profile of the normalized temperature fluctuation variance $\overline{\theta^2}$.

where $q^2 = u_i u_i$, lower cases represent fluctuating fields, and upper cases indicate the mean values; c_8, c_{10}, c_{11}, c_* are constants discussed in the following; τ_3 and τ_θ are characteristic times scales whose value will be determined in section 3; $\lambda_i = g_i\alpha$ where $g_i = (0, 0, g)$ is the gravitational acceleration; and α is the thermal expansion coefficient. The above equations do not include rotation and viscosity terms since their contributions to the TOMs are negligible in the atmospheric boundary layer.

In the present work, the TOMs are evaluated using mean flow and second order moments as input of the model. The vertical profiles are taken from the LES performed by Moeng and Sullivan (1994), who provided all the second-order moments (except for $\overline{uv}$, $\overline{\theta u}$, $\overline{\theta v}$, $\overline{\theta w}$, $\overline{\theta^2}$) and the variances vertical fluxes ($\overline{u^2 w}$, $\overline{v^2 w}$, $\overline{w^3}$) together with the mean flow components.

Concerning the missing second-order moments, for $\overline{\theta w}$ and $\overline{\theta^2}$, whose quite standard trend is well known in literature, we constructed the profiles reported in Figs. 1 and 2, similar to those shown in Canuto et al. (1994) in the case of the buoyancy-dominated BL. Since general profiles of $\overline{uv}$, $\overline{\theta u}$, $\overline{\theta v}$ are not available in literature we solved for them the following dynamic equations:

$$\frac{\partial \overline{uv}}{\partial t} = -\left(\overline{vw}\frac{\partial U}{\partial z} + \overline{uw}\frac{\partial V}{\partial z}\right) - \frac{\partial}{\partial z}\overline{uvw} - \Pi_{uv} \quad (6)$$

$$\frac{\partial \overline{\theta u}}{\partial t} = -\overline{uw}\frac{\partial \Theta}{\partial z} - \overline{\theta w}\frac{\partial U}{\partial z} - \frac{\partial}{\partial z}\overline{\theta uw} - \Pi_{\theta u} \quad (7)$$

$$\frac{\partial \overline{\theta v}}{\partial t} = -\overline{vw}\frac{\partial \Theta}{\partial z} - \overline{\theta w}\frac{\partial V}{\partial z} - \frac{\partial}{\partial z}\overline{\theta vw} - \Pi_{\theta v}, \quad (8)$$

where the pressure correlation terms Π_{uv}, $\Pi_{\theta u}$, and $\Pi_{\theta v}$ were prescribed as in Canuto (1992).

The Moeng and Sullivan (1994) case B LES considered here, starts with a laminar flow with an initial mean potential temperature stable profile that then becomes unstable during the simulation, keeping thermal inversion at the top. For this reason, in this case, we have used as input of the TOM model a temperature vertical profile similar to those of the LES final situation in which the turbulence moments were calculated. The mean potential temperature (Fig. 3) shows a slightly linear decreasing profile that begins to increase near the top of the BL.

The surface heat flux was set to $Q_* = (\overline{\theta w})_0 = 0.24$ (m s^{-1} K) and the convective velocity $w_* = [(g/T_0)Q_* Z_i]^{(1/3)} = 2.02$ (m s^{-1}) where g/T_0 is the buoyancy coefficient and Z_i is the PBL height; the temperature scale is $\theta_* = Q_*/w_*$. The values of the constants that appear in the dynamic equations are reported in Table 1. The value of c_{10} is taken from Canuto (1992), while c_* is a value taken between that suggested by Lumley et al. (1978), $c_* = 1$, and that of André et al. (1982), $c_* = 0$. The constants c_4 and c_6, in Table 1, are present in the pressure correlation terms (not shown) of the second-order moments equations used to calculate the missing profiles of $\overline{uv}$, $\overline{\theta u}$, and $\overline{\theta v}$ [Eqs. (6), (7), (8)]. Their values are slightly different to those suggested in Canuto (1992), $c_4 = 1.75$ and $c_6 = 3.75$. The value of c_{11} is larger than the standard used for this constant (e.g., Canuto 1992) so as to correctly simulate the buoyancy contribution. The value of the constant c_8 will be largely discussed in the following section.

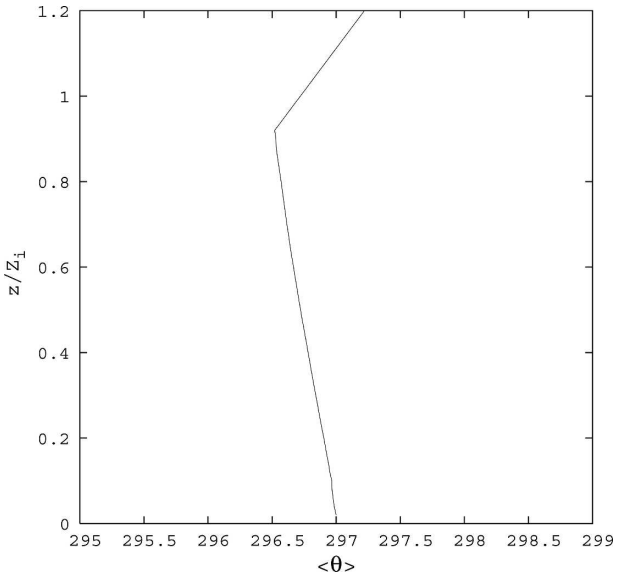

FIG. 3. Vertical profile of mean potential temperature.

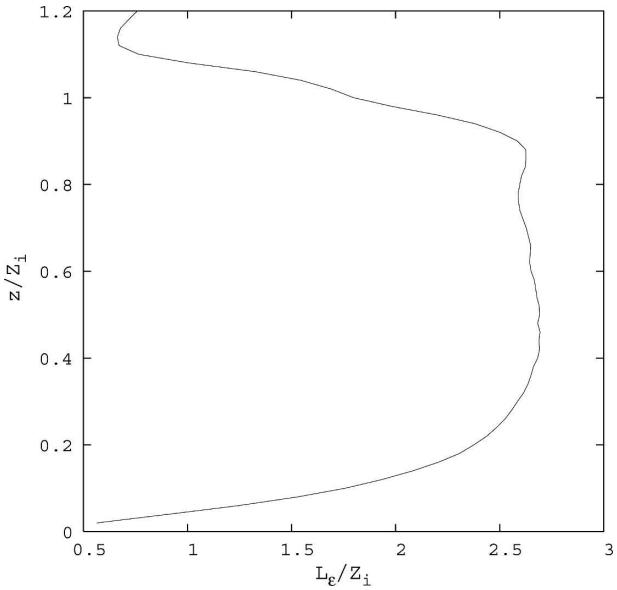

FIG. 4. Vertical profile of the normalized integral length scale for the dissipation rate from LES case B data.

The equations were numerically solved on a 60-level vertical grid using a centered finite differences scheme for derivatives in space and a forward difference scheme for derivatives in time. No boundary conditions were required.

3. Turbulent damping

Since the dynamic equations for the TOMs, as seen in the previous section, involve the fourth-order moments (FOMs), the treatment of the latter plays a key role in describing the nonlocal features of the flow, which are represented by the fluxes of the fluxes (TOMs). The most common and widely used closure for the FOMs is the quasi-normal approximation [QN; Eq. (1); see, e.g., Tatsumi 1957; Ogura 1972; Zeman and Lumley 1976; André et al. 1976, 1978; Canuto et al. 1994, 2001]. As has been recently demonstrated (Cheng et al. 2005) this approximation could not provide sufficient damping for the TOMs, which became arbitrarily large while in reality they have finite values. To limit this unphysical growth many approaches were suggested, such as the clipping approximation (André et al. 1976) and the Eddy-Damped Quasi-Normal Markovian (EDQNM) model (Orszag 1977; Lesieur 1992) in which the damping is represented by an additional time scale chosen on physical grounds.

TABLE 1. Model constant values.

c_6	c_{11}	c_4	c_{10}	c_*
3.5	0.9	1.5	6	0.4

In this paper we adopt the QN approximation but we propose a new method for the damping. As discussed in detail by Zeman (1981), the FOMs are taken to be distributed in accordance with a normal probability density but the pressure correlation terms are parameterized by third order terms divided by a time scale, usually denoted by τ_3. Lumley et al. (1978), demonstrated that this approximation is physically equivalent to the EDQNM model (Orszag, 1977; Lesieur, 1992).

On the lhs of Eqs. (2), (3), (4), and (5) the second and the third terms derive from the third-order pressure correlations, here parameterized following André et al. (1982). These terms, in which appear the time scale τ_3 and the analogous τ_θ, are essentially connected to the turbulent damping of the TOMs. Therefore, a proper choice of τ_3 and τ_θ can avoid the unphysical growth of the TOMs (Canuto et al. 2001). Both τ_3 and τ_θ depend on the characteristic turbulence life time τ:

$$\tau_3 = \frac{\tau}{2c_8} \quad \text{and} \quad \tau_\theta = \frac{\tau}{2c_2}, \tag{9}$$

where $\tau = 2e/\epsilon$, $e = (\overline{q^2}/2)$ is the turbulent kinetic energy, and ϵ is its mean dissipation rate. Thus the constants c_8 and c_2 should be chosen accurately and on physical ground, as in Canuto et al. (2001) and Ferrero (2005) in order to obtain the proper turbulence damping. The values of c_8 and c_2 are usually chosen constant (André et al. 1982; Canuto 1992).

Since the size of the eddies in the BL vary with the height, as shown in Fig. 4 where the length scale

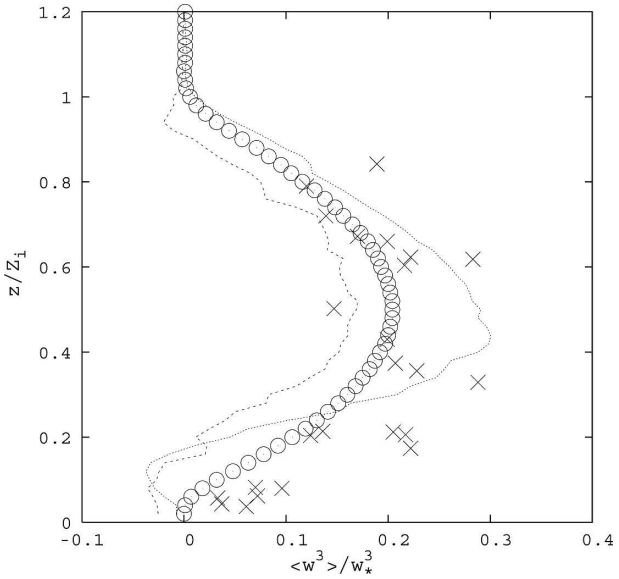

FIG. 5. Normalized vertical profile of $\overline{w^3}$ for case B. Comparison between TOM model with constant values of c_8 and c_2, where the dashed line represents $c_8 = 10$, $c_2 = 5$; and the dotted line represents $c_8 = 9.5$, $c_2 = 4.5$, LES (○ symbols), and aircraft data (× symbols) are shown.

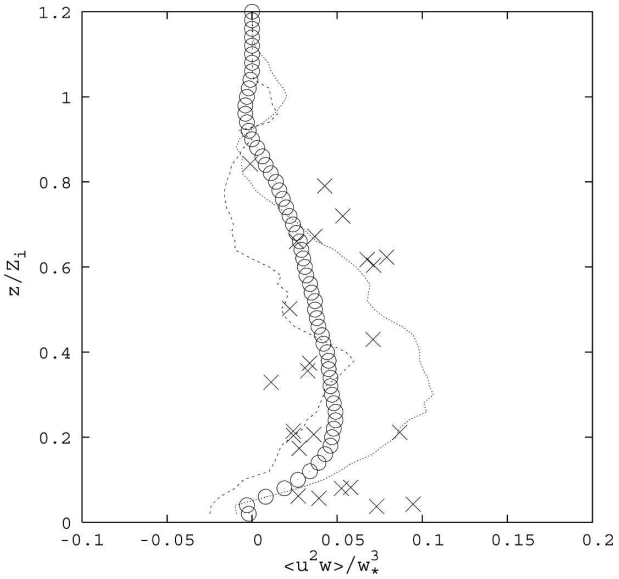

FIG. 6. Same as Fig. 5 except for $\overline{u^2w}$.

$L_\epsilon = [\overline{q^2}^{(3/2)}/\epsilon]$ obtained from Moeng and Sullivan (1994) LES data (case B) is reproduced, the turbulence damping should be different at different levels. Thus the value of c_8 and c_2 can be set as functions of the ratio L_ϵ/Z_i and estimated as follows:

$$c_8 = c_8^{\mathrm{A}}\left(1 + \frac{L_\epsilon}{c_8^{\mathrm{A}} Z_i}\right) \tag{10}$$

$$c_2 = c_2^{\mathrm{C}}\left(1 + \frac{L_\epsilon}{c_2^{\mathrm{C}} Z_i}\right), \tag{11}$$

where c_8^{A} and c_2^{C} are the values suggested by André et al. (1982) and Canuto (1992), respectively, ($c_8^{\mathrm{A}} = 8$ and $c_2^{\mathrm{C}} = 2.5$).

These expressions can be regarded as a first order correction to the c_8^{A} and c_2^{C} constant. We consider a linear dependence on the L_ϵ/Z_i ratio. As a matter of fact, quadratic dependence could give too large values, completely different from those available from literature. We are looking for a slight modulation of the constant based on physical ground. It can be also noted that the factor L_ϵ/Z_i is always positive being defined through two length scales.

4. Results

First we considered the buoyancy-dominated flow with a relatively small shear effect (Moeng and Sullivan 1994, case B). Following Ferrero (2005), we performed a first simulation in which the values of c_8 and c_2 were chosen constant. Taking into account that the maximum of L_ϵ is about $2.6Z_i$ (Fig. 4), we set $c_8 = 10$ and $c_2 = 5$. The results, shown in Figs. 5, 6, 7, and 8 (dashed line) demonstrate that with this values for the constants the TOMs are largely underestimated in the lower layers and near the top of the BL. Choosing slightly smaller values for the two constants ($c_8 = 9.5$ and $c_2 = 4.5$) the TOMs vertical profiles (dotted line) are improved in the bottom and top levels of the BL but show overestimation in the middle of the BL. For small val-

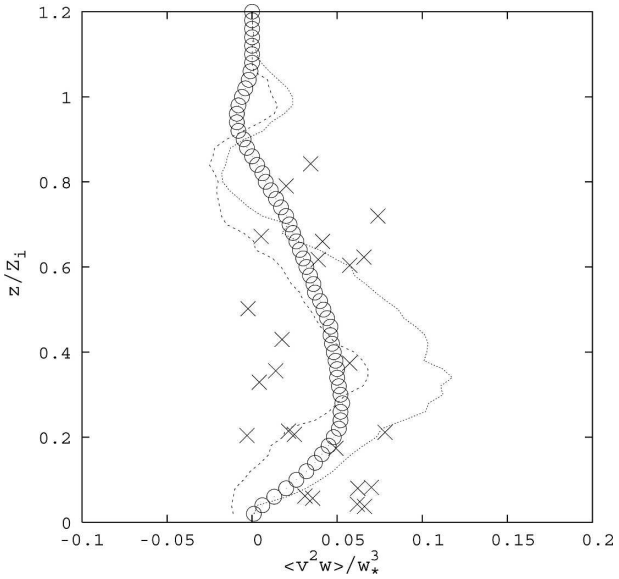

FIG. 7. Same as Fig. 5 except for $\overline{v^2w}$.

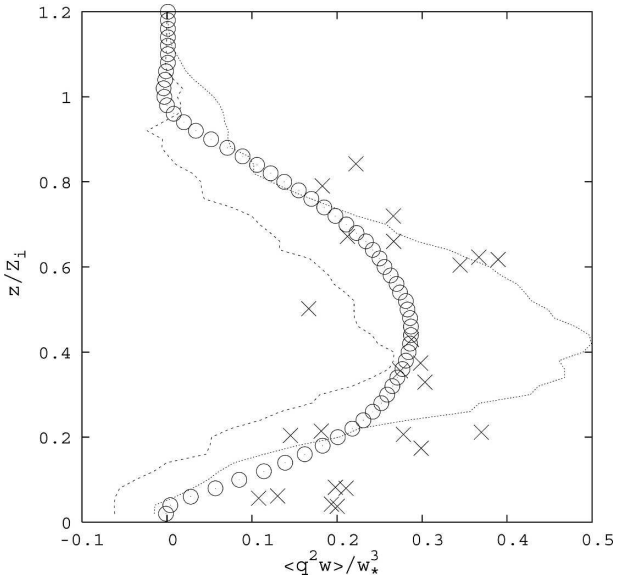

FIG. 8. Same as Fig. 5 except for $\overline{q^2w}$.

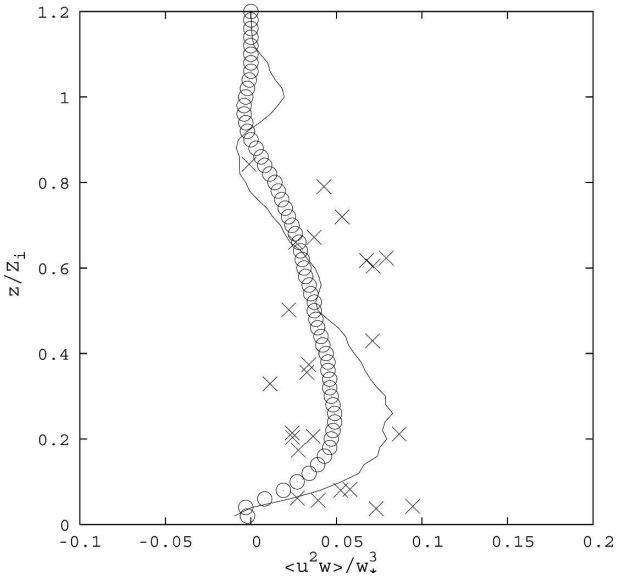

FIG. 10. Same as Fig. 9 except for $\overline{u^2w}$.

ues of c_8 and c_2 [as those suggested by André et al. (1982) and Canuto (1992)] the vertical profiles are excessively overestimated at the BL intermediate levels, while for large values of the constants they show underestimation in the upper and lower layers.

These results suggest that, as discussed in the previous section, the constants c_8 and c_2, which are responsible for the turbulent damping, cannot be taken constant throughout the whole BL. For this reason we performed a new simulation calculating c_8 and c_2 at each level as a function of the length scale L_ϵ from Eqs. (10) and (11).

The resulted TOMs are depicted in the following figures together with the LES data (Moeng and Sullivan 1994), where available, and aircraft measurements (Hartmann et al. 1999). Figures 9, 10, 11, and 12 show the normalized vertical profiles of the three variances fluxes and the resulting turbulent kinetic energy vertical flux. Generally the agreement of the simulated TOMs is satisfactory as is shown by the $\overline{q^2w}$ vertical profile, which reproduces well both the LES data and

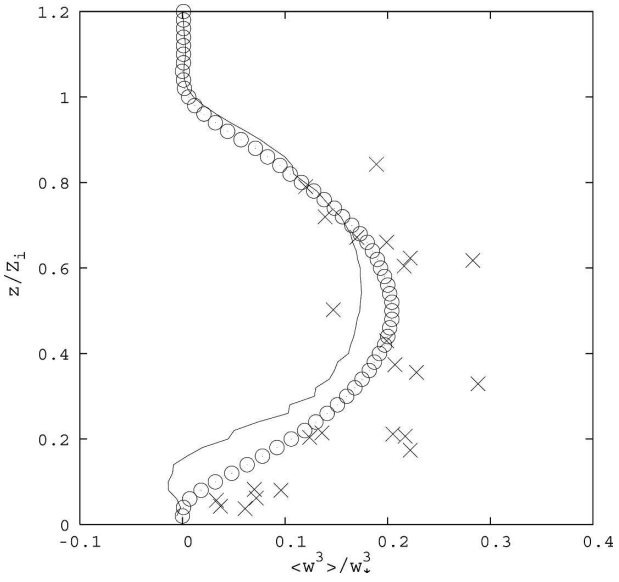

FIG. 9. Normalized vertical profile of $\overline{w^3}$ for case B. Comparison between TOM model (solid line), LES (○), and aircraft data (×).

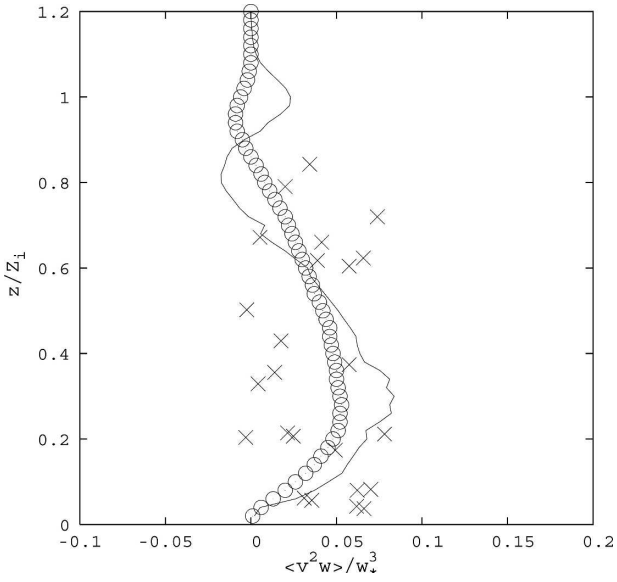

FIG. 11. Same as Fig. 9 except for $\overline{v^2w}$.

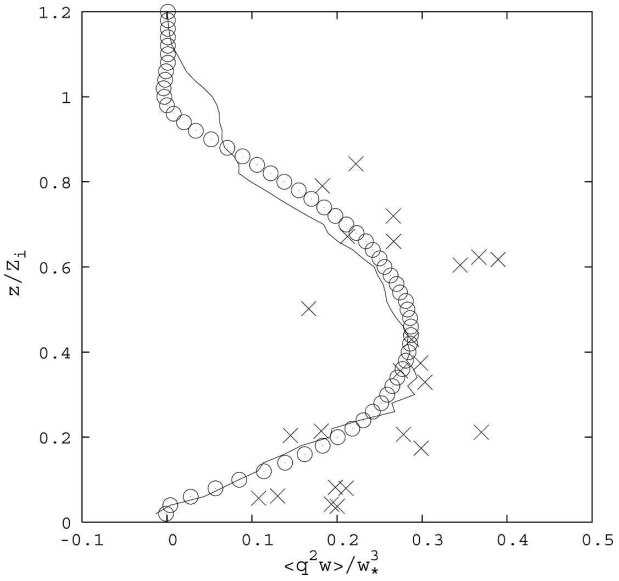

FIG. 12. Same as Fig. 9 except for $\overline{q^2w}$.

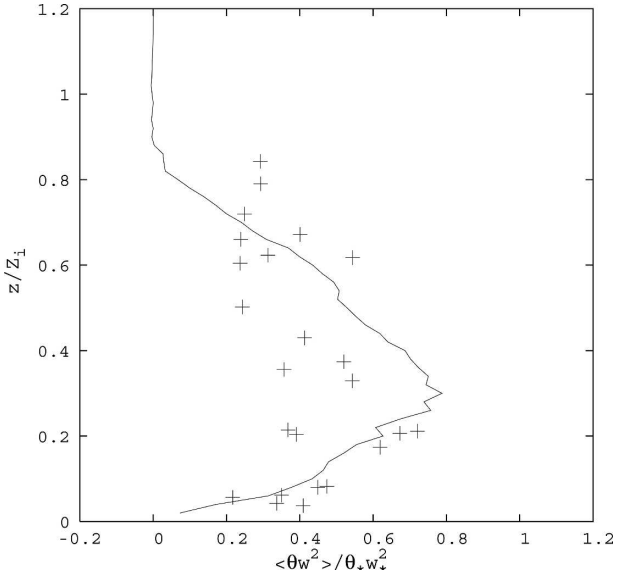

FIG. 14. Same as Fig. 13 except for $\overline{\theta w^2}$.

the aircraft measurements. Nevertheless it can be noted that the $\overline{w^3}$ vertical profile is slightly underestimated in the lower part of the BL while an opposite behavior occurs for the $\overline{u^2w}$ and $\overline{v^2w}$ vertical profiles. This fact suggests that the model is able to correctly simulate the turbulence production and transport, while is not completely satisfactory in the redistribution along the different components.

In Figs. 13, 14, and 15 the normalized vertical profiles of $\overline{\theta^2w}$, $\overline{\theta w^2}$, and $\overline{\theta^3}$ are compared with the aircraft measurements only, as in this case the LES data were not available. The agreement is particularly good for $\overline{\theta^3}$ and $\overline{\theta w^2}$, while $\overline{\theta^2w}$ is underestimated near the ground where the simulated profile decrease similarly to that found by Cheng et al. (2005).

To verify our approach and in particular the proposed method for the damping on a wide range of atmospheric conditions, we applied the TOM model to the case SB1 of Moeng and Sullivan (1994). This case is

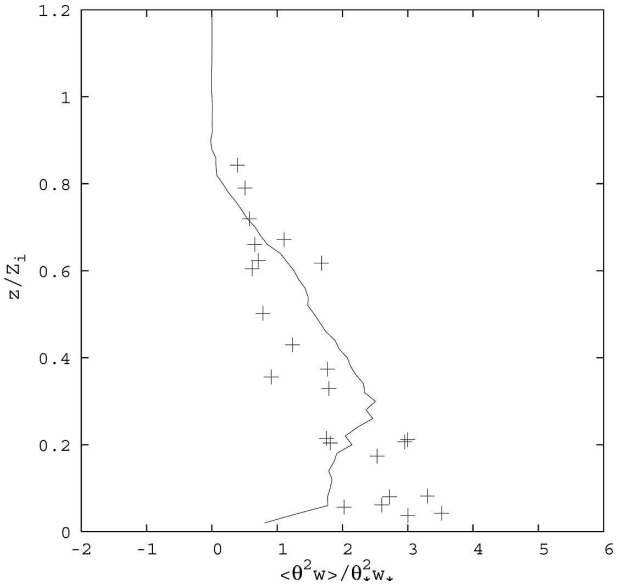

FIG. 13. Normalized vertical profile of $\overline{\theta^2w}$ for case B. Comparison between TOM model (solid line) and aircraft data (+).

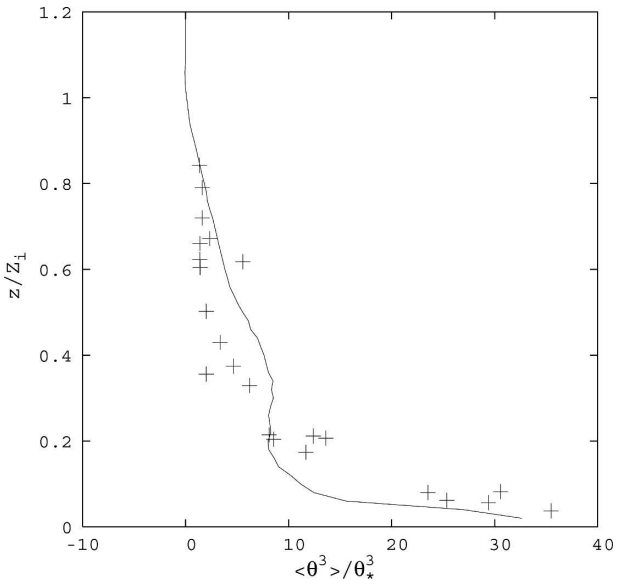

FIG. 15. Same as Fig. 13 except for $\overline{\theta^3}$.

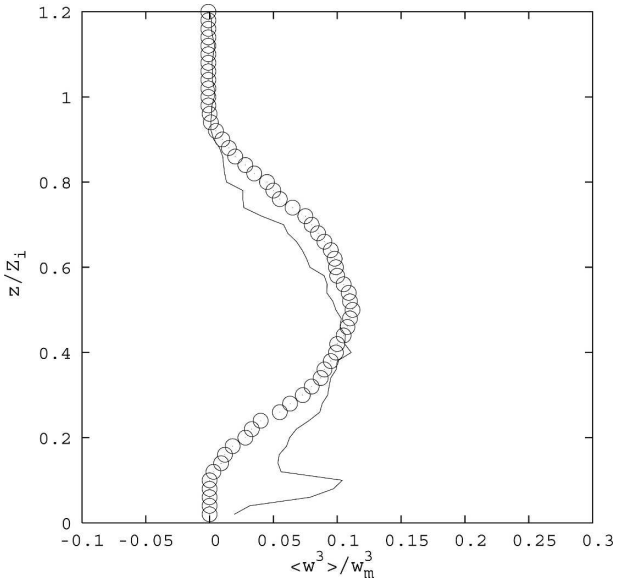

FIG. 16. Normalized vertical profile of $\overline{w^3}$ for case SB1. Comparison between TOM model (solid line) and LES (○).

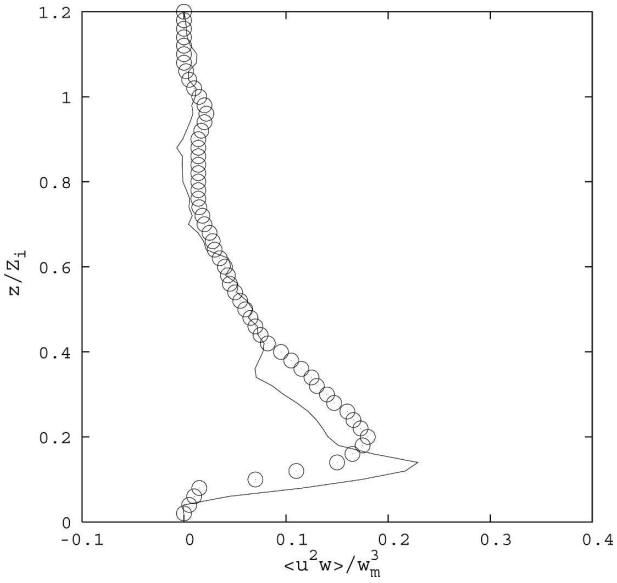

FIG. 17. Same as Fig. 16 except for $\overline{u^2w}$.

characterized by a value of $z_i/L = 1.5$, $Q_* = (\overline{\theta w})_0 = 0.05$ (m s^{-1} K) and $w_* = [(g/T_0)Q_*Z_i]^{(1/3)} = 0.94$ (m s^{-1}), which correspond to a BL where both shear and buoyancy contribute nearly equally. As for the simulation of the case B, we evaluated the TOMs using mean flows and second order moments as input of the model. Most of the vertical profiles were provided by Moeng and Sullivan (1994); the missing second-order moments ($\overline{uv}$, $\overline{\theta u}$, $\overline{\theta v}$) were evaluated by solving their dynamic equations [see Eqs. (6), (7), and (8)], while the profile of $\overline{\theta^2}$ was deduced from literature, as done for the case B. Concerning the vertical profile of the mean potential temperature we taken into account that a small amount of buoyancy forcing can effectively mix the mean flows in the middle of the BL and therefore the profile used in input of the model was characterized by a constant trend in the middle of the BL with a weak instability near the ground and a capping inversion at the upper layers. The constant c_8 and c_2 were prescribed by Eqs. (10) and (11) and the corresponding L_ϵ profile for the case SB1.

The results of the simulation are shown in Figs. 16, 17, 18, and 19, where the TOMs predicted by our model are compared with LES results. Following Moeng and Sullivan (1994), the TOMs are normalized by the velocity scale for the shear-buoyancy-driven BL defined as $w_m^3 = w_*^3 + 5u_*^3$, ($u_* = 0.59$ m s^{-1}). Also in this simulation the agreement between model results and LES data is satisfactory. Concerning $\overline{w^3}$ (and consequently $\overline{q^2w}$) profile, it can be noted that the agreement with LES data is less satisfactory in the lowest layer where it presents a maximum not shown in the LES data. This is due to some features of the input variable profiles, in particular the strong negative gradient of $\overline{w^2}$ near the ground. These results demonstrate that our model and the proposed method for the TOMs damping can be applied to a wide range of BL flows.

5. Conclusions

In this work we present a turbulence model accounting for TOMs in a BL with both convection and shear.

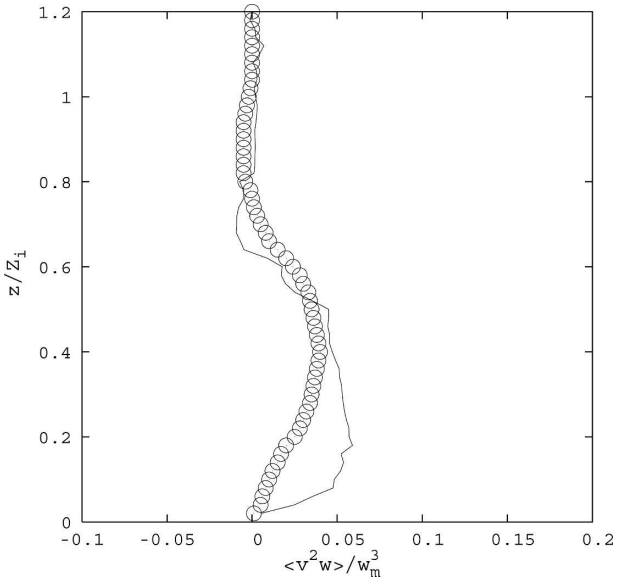

FIG. 18. Same as Fig. 16 except for $\overline{v^2w}$.

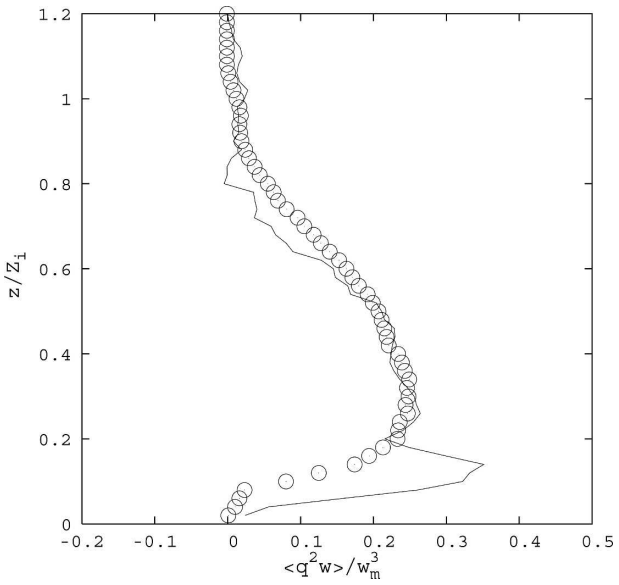

FIG. 19. Same as Fig. 16 except for $\overline{q^2 w}$.

The model we consider is based on the Canuto (1992) paper in which the FOMs are closed with the QN approximation. As it is generally recognized (Cheng et al. 2005), this approximation needs a proper turbulent damping in order to avoid the unphysical growth of the TOMs. This problem is solved in this work prescribing variable values for the constant c_8 and c_2, according to the vertical profile of the integral length scale of the turbulence. The TOMs calculated with this model are compared with LES data (Moeng and Sullivan 1994, case B) and aircraft measurements (Hartmann et al. 1999). The results show a satisfactory agreement for all the TOMs considered in both the cases, thus demonstrating that the turbulent damping should depend on the turbulence length scale that is a measurement of the eddy size that can grow in different ways at the different levels of the BL. The test is more significant because, together with LES data, atmospheric measurements (as those provided by Hartmann et al. 1999) are used for comparison. As a matter of fact, the TOMs profiles obtained from LES can be slightly different, even showing the same basic features, depending on the code used (as assessed by Fedorovich et al. 2004).

To cover all the possible atmospheric conditions, other cases characterized by different values of the Monin–Obukov length, should be considered. As a matter of fact, the roles played by buoyancy and shear respectively may be different (see, e.g., Fedorovich et al. 2004). For this reason, we successfully tested our model and the new damping method in the case of shear and buoyancy driven BL (Moeng and Sullivan 1994, case SB1).

Furthermore, this paper points out the importance of a proper choice of the turbulent time scales based on physical ground to correctly simulate the vertical fluxes of the wind velocity and temperature fluctuation variances, which are responsible for the nonlocal transport. Finally, we would like to stress that the model here presented is able to account for both the turbulence production processes, namely shear and buoyancy, at the same time and that such a complex situation corresponds to the actual atmospheric BL.

Acknowledgments. The authors thank V. M. Canuto for his useful suggestions, and V. M. Gryanik and J. Hartmann for kindly providing us with the aircraft data.

REFERENCES

Abdella, K., and N. McFarlane, 1997: A new second-order turbulence closure scheme for the planetary boundary layer. *J. Atmos. Sci.,* **54,** 1850–1867.

André, J. C., G. De Moor, P. Lacarrere, and R. du Vachat, 1976: Turbulence approximation for inhomogeneous flows. Part I: The clipping approximation. *J. Atmos. Sci.,* **33,** 476–481.

——, ——, ——, G. Therry, and R. du Vachat, 1978: Modelling the 24 h evolution of the mean and turbulent structures of the planetary boundary layer. *J. Atmos. Sci.,* **35,** 1861–1883.

——, P. Lecarre, and K. Traore, 1982: Pressure effects on triple correlations in turbulent convective flows. *Turbulent Shear Flow,* Vol. 3, Springer, 243–252.

Canuto, V. M., 1992: Turbulent convection with overshooting: Reynolds stress approach. *Astrophys. J.,* **392,** 218–318.

——, and Y. Cheng, 1994: Stably stratified shear turbulence: A new model for the energy dissipation length scale. *J. Atmos. Sci.,* **51,** 2384–2396.

——, F. Minotti, C. Ronchi, R. M. Ypma, and O. Zeman, 1994: Second-order closure PBL model with new third-order moments: Comparison with LES data. *J. Atmos. Sci.,* **51,** 1605–1618.

——, Y. Cheng, and A. Howard, 2001: New third-order moments for the convective boundary layer. *J. Atmos. Sci.,* **58,** 1169–1172.

——, ——, and ——, 2002: An improved model for the turbulent PBL. *J. Atmos. Sci.,* **59,** 1550–1565.

——, ——, and ——, 2005: What causes the divergences in local second-order models? *J. Atmos. Sci.,* **62,** 1645–1651.

Cheng, Y., V. M. Canuto, and A. M. Howard, 2005: Nonlocal convective PBL model based on new third- and fourth-order moments. *J. Atmos. Sci.,* **62,** 2189–2204.

Deardorff, J. W., 1972: Theoretical expression for the countergradient vertical heat flux. *J. Geophys. Res.,* **77,** 5900–5904.

Fedorovich, E., and Coauthors, 2004: Entrainment into sheared convective boundary layers as predicted by different large eddy simulations codes. Preprints, *16th Symp. on Boundary Layer and Turbulence,* Portland, ME, Amer. Meteor. Soc., CD-ROM, P4.7.

Ferrero, E., 2005: Third-order moments for shear driven boundary layers. *Bound.-Layer Meteor.,* **116,** 461–466.

——, and M. Racca, 2004: The role of the nonlocal transport in modelling the shear-driven atmospheric boundary layer. *J. Atmos. Sci.,* **61,** 1434–1445.

Gryanik, V. M., and J. Hartmann, 2002: A turbulence closure for the convective boundary layer based on a two-scale mass-flux approach. *J. Atmos. Sci.,* **59,** 2729–2744.

——, ——, S. Raasch, and M. Schroter, 2005: A refinement of the Millionschikov quasi-normality hypothesis for convective boundary layer turbulence. *J. Atmos. Sci.,* **62,** 2632–2638.

Hanjalic, K., and B. Launder, 1972: A Reynold stress model of turbulence and its application to thin shear flows. *J. Fluid Mech.,* **52,** 609–638.

——, and ——, 1976: A contribution towards Reynold-stress closure for low-Reynolds-number turbulence. *J. Fluid Mech.,* **74,** 593–610.

Hartmann, J., and Coauthors, 1999: Arctic Radiation and Turbulence Interaction Study (ARTIST). Rep. 305 on Polar Research, Alfred Wegener Institute for Polar and Marine Research, Bremerhaven, Germany, 81 pp.

Holstag, A. A. M., and C. H. Moeng, 1991: Eddy diffusivity and countergradient transport in the convective atmospheric boundary layer. *J. Atmos. Sci.,* **48,** 1690–1700.

——, and B. A. Boville, 1993: Local versus nonlocal boundary layer diffusion in a global climate model. *J. Climate,* **6,** 1825–1842.

Lenschow, D. H., 1974: Model of the height variation of the turbulence kinetic energy budget in the unstable planetary boundary layer. *J. Atmos. Sci.,* **31,** 465–474.

——, J. C. Wyngaard, and W. T. Pennell, 1980: Mean-field and second-moment budgets in a baroclinic convective boundary layer. *J. Atmos. Sci.,* **37,** 1313–1326.

Lesieur, M., 1992: *Turbulence in Fluids*. Kluwer Academic, 412 pp.

Lumley, J. L., O. Zeman, and J. Siess, 1978: The influence of buoyancy on turbulent transport. *J. Fluid Mech.,* **84,** 581–597.

Mellor, G. L., and T. Yamada, 1974: A hierarchy of turbulence closure models for planetary boundary layers. *J. Atmos. Sci.,* **31,** 1791–1806.

——, and ——, 1982: Development of a turbulence closure model for geophysical fluid problems. *Rev. Geophys. Space Phys.,* **20,** 851–875.

Moeng, C. H., and J. C. Wyngaard, 1989: Evaluation of turbulent transport and dissipation closures in second-order modeling. *J. Atmos. Sci.,* **46,** 2311–2330.

——, and R. Rotunno, 1990: Vertical velocity skewness in the buoyancy-driven boundary layer. *J. Atmos. Sci.,* **47,** 1149–1162.

——, and P. Sullivan, 1994: A comparison of shear- and buoyancy-driven planetary boundary layer flows. *J. Atmos. Sci.,* **51,** 999–1022.

Ogura, Y., 1962: Energy transfer in isotropic turbulent flow. *J. Geophys. Res.,* **67,** 3143–3149.

Orszag, S., 1977: Statistical theory of turbulence. *Fluid Dynamics,* R. Balian and J. L. Peube, Eds., Gordon and Breach, 237–374.

Tatsumi, T., 1957: The theory of decay process of incompressible isotropic turbulence. *Proc. Roy. Soc. London,* **A239,** 16–45.

Trini Castelli, S., E. Ferrero, and D. Anfossi, 2001: Turbulence closure in neutral boundary layers over complex terrain. *Bound.-Layer Meteor.,* **100,** 405–419.

Wyngaard, J. C., and J. C. Weil, 1991: Transport asymmetry in skewed turbulence. *Phys. Fluids,* **A3,** 155–162.

Zeman, O., 1981: Progress in the modelling of planetary boundary layers. *Annu. Rev. Fluid. Mech.,* **13,** 253–272.

——, and J. L. Lumley, 1976: Modeling buoyancy driven mixed layers. *J. Atmos. Sci.,* **33,** 1974–1988.

Zilitinkevich, S., V. M. Gryanik, V. N. Lykossov, and D. V. Mironov, 1999: Third-order transport and nonlocal turbulence closures for convective boundary layers. *J. Atmos. Sci.,* **56,** 3463–3477.